*Proceedings of MARTEC 2010*
*The International Conference on Marine Technology*
*11-12 December 2010, BUET, Dhaka, Bangladesh*

# AERODYNAMIC CHARACTERISTICS OF A COMPOUND WING DURING GROUND EFFECT

**Saeed-Jame, Adi-Maimun, Agoes-Priyanto, Nor-Azwadi**

Department of Marine Technology, Faculty of Mechanic Engineering
Universiti Teknologi Malaysia (UTM)Skudai, Johor, Malaysia
E-mail: jsaeed2@live.utm.my

## ABSTRACT

*The paper numerically investigated the flow characteristics over a compound wing during ground effect. The compound wing is divided into three parts where one rectangular wing in the middle and two taper reverse wings with negative dihedral angle in sides. The NACA6409 airfoil was employed as section of wings. Three dimensional (3D) Computational Fluid Dynamic (CFD) was applied as a computational scheme. The k-ε turbulent model was utilized for characterization of flow over wing surface. The computational results of a rectangular wing with aspect ratio 1.5 and angle of attack 2° with different ground clearance were compared with experimental data of published work. Next, the principal aerodynamic characters of compound wing and a rectangular wing were computed for various ground clearance. The numerical results of CFD simulation of compound wing were compared with the rectangular wing and have an acceptable improvement in lift and drag ratio, although its stability a little reduced. The major modification of lift to drag ratio of compound wing occurs at extreme ground effect.*

**Key words**: Wing-in-ground effect, Compound wing, Aerodynamic characteristics, CFD model.

**Nomenclature**

| | |
|---|---|
| b | Wing Span |
| c | Chord length |
| $C_L$ | Lift Coefficient |
| $C_D$ | Drag Coefficient |
| $C_M$ | Moment coefficient |
| D | Drag Force |
| h | height of trailing edge above the ground |
| h/c | Ground clearance |
| k | Turbulent kinetic energy |
| L | Lift force |
| L/D | Lift to drag ratio |
| M | Pitching moment at c/4 from the leading edge |
| S | Reference area (= bc) |
| $S_{ij}$ | Mean rate of deformation tensor |
| U | Free stream mean velocity |
| $X_{CP}$ | Center of pressure from the leading edge |
| α | angle of attack |
| μ | Viscosity |
| $\mu_t$ | Turbulent viscosity |
| ε | Turbulent energy dissipation rate |
| ρ | air density |

## 1. INTRODUCTION

The wing-in- ground effect (WIG) crafts are classified as a middle form between ships and aircrafts. WIG crafts can fly proximity the any surface such as ground, sea, snow and ice etc. A high pressure air (air cushion) is generated from interface between wing of the WIG craft and the ground. The dropping of down-wash angle because of the ground effect guides to an enhancement in lift and decline of induce drag, with a raise of effective aspect ratio for the wing. Rising in the lift force and decreasing of induced drag provides an augmentation on the lift to drag ratio (L/D) [1]. The type of air cushion is the principal difference between hovercraft and WIG craft. A static air cushion holds hovercraft, while the WIG craft is borne by dynamic air cushion. The small aspect ratio of wing and high lift to drag ratio are other differences from a conventional craft. Currently, the suitable expansion of high power computing and computational fluid dynamic (CFD) grows the numerical aerodynamic characteristics of WIG crafts [2].

There are a lot of concepts of wing-in-ground effect. First time, the idea of ram wing was put into operation by Troeng [2]. Practically all WIG craft employ high pressure ram air for improved lift,

nevertheless the fault of ram wing WIG craft is its stability. According this concept a number of WIG craft included a low aspect ratio wing (approximately square) and a large horizontal tail installed out of ground effect which supplies the essential stability. The wing is often built-in endplates with the aim of increase ground effect. Tandem-Airfoil-Flairboat (TAF) is defined by the proposal of assembling two short wings in tandem. Both wings have roughly the same dimensions with rather small space in between and no horizontal tail. This arrangement presents good stability in extreme ground effect, but unstable when out of ground effect. A special class of ram wing called as Lippisch idea where the main wing includes an inverse dihedral wing along the leading edge. This design embraces more longitudinal stability rather than a low aspect ratio ram wing. A smaller horizontal tail is required for longitudinal stability requirement in low ground clearance and jump modes during cruise condition. The Lippisch concept uses a greater aspect ratio of wing rather than ram wing concept which get near to 3. The lift to drag ratio of Lippisch craft were around 25. The completed type of Lippisch craft is Airfish. This WIG craft generally flies on the proximity to the ground. The operational range ground clearance of Airfish craft is between 0.1m and 1 m. The design of Airfish is described for utilizing ground effect but it allows to dynamic jumps about 5 m in some transitory condition. The plan Hoverwing craft utilizes a plain system of flexible skirts to hold an air cushion between the twin hulls. This static air cushion is employed just through takeoff, therefore assisting the craft to accelerate with smallest power before shifting to true ground effect mode [2]. The Hydrofret concept is classified to use both static air cushion and dynamic ground effect. The concept is planned in two models. The first is a ram-wing catamaran balanced by a large aspect ratio forward wing tail. In the different description a large aspect ratio rear wing is employed instead the tail wing [2].

Chawla et al. [3] described Wing-in-ground effects from a wind-tunnel research of a NACA 4415 airfoil section for wing model with an aspect ratio of 2.33. They employed moveable flap and detachable end and center plates. They showed ground effect of wing is appeared for ground clearance (h/c) up to 1. The influence of endplate on lift to drag ratio is higher for lower ground clearance. Ahmed and Sharma [4] studied on the pressure distribution over the wing surface at different ground clearances and angles of attack for measuring the lift, drag and the mean flow over the surface of the wing, also they depicted the wake region for mean and fluctuating velocities of flow. The convergent–divergent passage shape between the wing and the ground at certain angle of attack gives a suction effect that causes a local reduction in lift. The higher lift force mostly related to adoption of pressure distribution on the lower surface of wing due to ground effect and increasing of pitching angle. They showed a thick wake region on suction surface at small ground clearance and high angle of attack. Because of merging the boundary layers of wing and ground plate in extreme ground effect especially at high angle the drag force has an enhancement. Ahmed et al. [5] studied the aerodynamic characteristics of NACA4412 airfoil section in a low turbulence wind tunnel with moving ground model at a Reynolds number of $3.0\times10^6$ by changeable the angle of attack from 0 to 10º and ground clearance (h/c) 0.05-1. They measured the pressure distribution, velocity and wake region of flow over the airfoil surface, also lift and drag forces. They showed a reduction of suction on upper surface when the airfoil come close to the ground for all pitch angle. Lift force reduces when decreasing ground clearance for small angle of attack ($\alpha<6º$), although it augmented for greater angle of attack by improvement pressure distribution on the pressure side. Further, they illustrated the drag force is higher in extreme ground effect due to transformation of the lower side pressure distribution. Jung et al. [6] performed extensive tests in the closed-type wind tunnel. Lift and drag forces and the pitch moment of NACA6409 were measured as main aerodynamic parameters such as the aspect ratio (AR), angle of attack ($\alpha$), ground clearance (h/c) and endplate shape were varied. They demonstrated the ground effect caused a decline in the tip vortex and the wake following the wing. The lift enhanced because of the ground effect at short ground clearance when the endplate is not fitted to wing. Due to the boundary layer that extends on extreme ground ($h/c< 0.1$), the lift force may possibly be a little underestimated. Also they proved by smoke trace test, the flow transitory under the pressure side is reserved by the endplate that causes a reduction on the tip vortex by the pressure difference between the pressure and suction sides of the wing. Furthermore, the influence of endplate on lift force for smaller aspect ratio of wing is grater than larger aspect ratio wing. The drag force is reduced by the ground effect when the wing moves toward the ground. The explanation is that the induced drag diminishes due to the drop of the tip vortex at the wing tip. Another finding of Jung et al. [6] is that when the angle of attack and the aspect ratio increased, the center of pressure shifted ahead to the leading edge of the wing. The center of pressure moved to the leading edge by adding an endplate to wing. As the ground clearance o decreased, the center of pressure also moved forward to the leading edge of wing.

The turbulent flow around two-dimensional wing was numerically investigated for fixed and moving ground boundary by Chun and Chang [7]. An incompressible Reynolds Average Navier-Stokes

(RANS) equation with finite difference method was applied for numerical model. According to their computational results, the difference in the lift and moment coefficients simulated by two bottom conditions is trivial, but the drag coefficient simulated by the fixed bottom is to some amount smaller than that by the moving one**.** Aerodynamic characteristics of three-dimensional wings in ground effect for Aero-levitation Electric Vehicle (AEV) are numerically investigated for various ground clearances and wing spans at the chord-length based Reynolds number of $2\times10^6$ by Moon et al. [8]. The design of AEV system is based on small wing span for decreasing costs of the structure and making of cruising channel. This system uses the tandem wing concept to satisfy the requirement lift. They showed the increasing of lift to drag ratio versus very low ground clearance (h/c<0.1) is nonlinear. Moreover, the lift to drag ratio for small span of AVD wings enhances between 10-40%. Ockfen and Matveev [9] researched numerically on airflow over NACA4412 airfoil section with favorable flap pattern that get better aerodynamic characteristics in extreme ground effect. The Spalart-Allmaras turbulence model of the Navier-Stokes equations via Fluent6.3 was used for various Reynolds number and angle of attack during ground effect. They depicted with small flap deflection the lift to drag ratio has a considerable enhancement, although for high flap angle the pressure drag increasing subsequently lift to drag ratio would be lesser than the wing without flap.

The lift to drag ratio of only wing decreases as other part add to wing [2]. Kirillovikh [10] reported the lift-to-drag ratio of a wing with aspect ratio 2–3 and ground clearance 0.2 would be about 35–45 that it is so large. When other part of crafts such as hull and pylon are included to wing, the reduction of lift-to-drag ratio arises consequently lift to drag ratio in this sample reach to 12-16.

The aim of this paper is aerodynamic characteristics of a compound wing during ground effect. The compound wing has been completed by three parts that a rectangular wing in the middle and two taper reverse wing with negative dihedral angle in sides. The numerical model used the three dimensional (3D) CFD using finite volume scheme. The standard k-ε turbulent model has been utilized for turbulent flow around wing. The numerical result of the present wing is compared with a rectangular wing.

## 2. CFD NUMERICAL STUDY

Present numerical study was carried out by a model of rectangular wing and compound wing with NACA6409 airfoil section. The principle dimensions of both wings (Figure 1(a)-1(b)) are shown in Table 1. These simulation were prepared with respect to different ground clearance (h/c= 0.1 ,0.15, 0.2, 0.25, 0.3), angle of attack 2°, aspect ratio 1.5 for validation and 1.25 for present model and velocity of airflow 30.8 m/s (60 knots). Ground clearance (h/c) is defined of the distance ratio between wing trailing edge and ground surface (h) to wing chord length (c). The numerical scheme considered a steady –state, incompressible by means of *k-ε* turbulent model of the Navier-Stokes equations for flow over wing surface. The CFD models applied Fluent 6.3 software and high speed computer. The transport equations for the turbulent kinetic energy (*k*) and turbulent dissipation energy (*ε*) are expressed as follows.

$$\frac{\partial(\rho k)}{\partial t}+div(\rho kU)=div\left[\frac{\mu_t}{\sigma_k}grad(k)\right]+2\mu_t S_{ij}\cdot S_{ij}-\rho\varepsilon \quad (1)$$

$$\frac{\partial(\rho\varepsilon)}{\partial t}+div(\rho\varepsilon U)=div\left[\frac{\mu_t}{\sigma_\varepsilon}grad(\varepsilon)\right]+C_{1\varepsilon}\frac{\varepsilon}{k}2\mu_t S_{ij}\cdot S_{ij}-C_{2\varepsilon}\rho\frac{\varepsilon^2}{k} \quad (2)$$

where $\mu_t$ is turbulent viscosity.

$$\mu_t=\rho C_\mu\frac{k^2}{\varepsilon} \quad (3)$$

The adaptable constants $C_\mu$, $\sigma_k$, $\sigma_\varepsilon$, $C_{1\varepsilon}$ and $C_{2\varepsilon}$ have the following values:

$C_\mu$= 0.09 σk = 1.00 $\sigma_\varepsilon$= 1.3 $C_{1\varepsilon}$= 1.44 $C_{2\varepsilon}$ =1.92.

The aerodynamic coefficients and center of pressure in this numerical study were determined as follows:

$C_L=\frac{L}{0.5\rho U^2 S}, C_D=\frac{D}{0.5\rho U^2 S}, C_M=\frac{M}{0.5\rho U^2 Sc}$ and

$X_{CP}=0.25+\frac{C_M}{C_L\cos\alpha+C_D\sin\alpha}$.

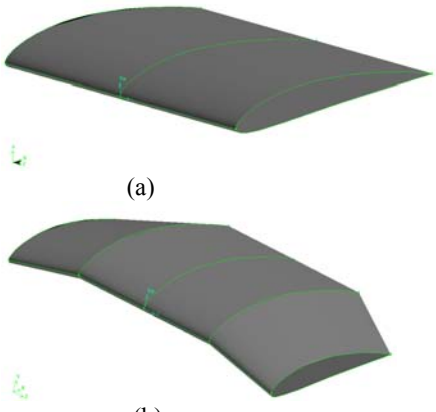

(a)



(b)

Figure 1: (a) The rectangular wing, (b) the compound wing.

Table 1: Principle dimension of wings.

| | |
|---|---|
| Total wing span (b) | 83.4 cm |
| Chord length (c) | 66.7 c m |
| Middle wing span | 41.4 cm |
| Taper ratio | 0.8 |
| Dihedral angle | 13º |

The number of mesh for each simulation is about 4,000,000-4,500,000. The $y^+$ values for turbulent is less than 100. This number of elements has good enough convergence for aerodynamic characteristics. The present simulation used symmetry plan as shown Figure 2 for ram wing and Figure 3 for compound wing. This is to shorten the simulation time although the results achieved will be the same.

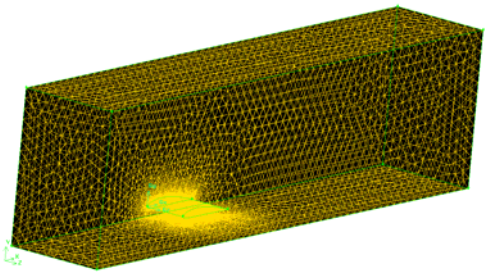

Figure 2: The meshing of rectangular wing.

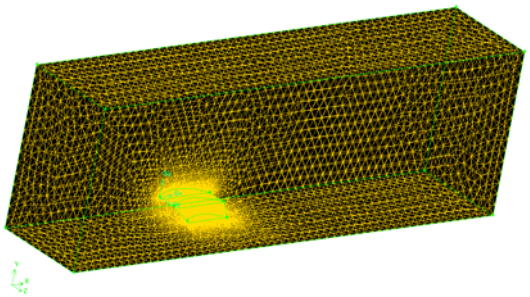

Figure 3: The meshing of compound wing.

## 3. VALIDATION OF CFD SIMULATION

The experimental results of Jung et al. [6] are taken to validate the present CFD simulation. The accuracy of numerical aerodynamic characters such as lift coefficient, drag coefficient, lift to drag ratio, moment coefficient and center of pressure were compared with experimental results. For validation purpose, the numerical results of a rectangular wing with NACA 6409 airfoil section were proved.

### 3.1 Lift Coefficient ($C_L$)

The present numerical results and experimental data [6] of lift coefficient were summarized in Table 2. Figure 4 depicts a comparison of lift coefficient for different ground clearance with aspect ratio 1.5 and pitch angle 2º. This figure shows a good agreement between computational and experimental results. The trend of both results illustrates a growth of lift coefficient when ground clearance decreases.

Table 2: Lift coefficient versus ground clearance with angle of attack 2º and AR = 1.5 for experimental and numerical result.

| Ground clearance | Numerical | Experimental |
|---|---|---|
| 0.1 | 0.3741 | 0.3980 |
| 0.15 | 0.3566 | 0.3930 |
| 0.2 | 0.3418 | 0.3682 |
| 0.25 | 0.3389 | 0.3682 |
| 0.3 | 0.3286 | 0.3682 |

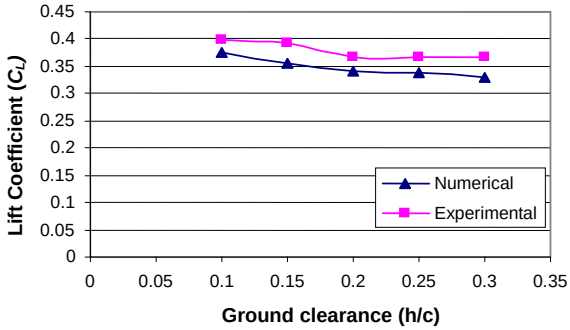


Figure 4: Lift coefficient ($C_L$) versus ground clearance (h/c) for angle of attack 2º and AR = 1.5.

### 3.2 Drag Coefficient ($C_D$)

The computational results and experimental data [6] of drag coefficients were listed in Table 3. The tendency of both results has good agreement but the computational results are a slight greater as shown in Figure 5. The increment of drag coefficient due to increasing of ground clearance was established by numerical and experimental scheme.

Table 3: Drag coefficient versus ground clearance with angle of attack 2º and AR = 1.5 for experimental and numerical result.

| Ground clearance | Numerical | Experimental |
|---|---|---|
| 0.1 | 0.0384 | 0.0308 |
| 0.15 | 0.0408 | 0.0308 |
| 0.2 | 0.0415 | 0.0348 |
| 0.25 | 0.0425 | 0.0328 |
| 0.3 | 0.0424 | 0.0348 |

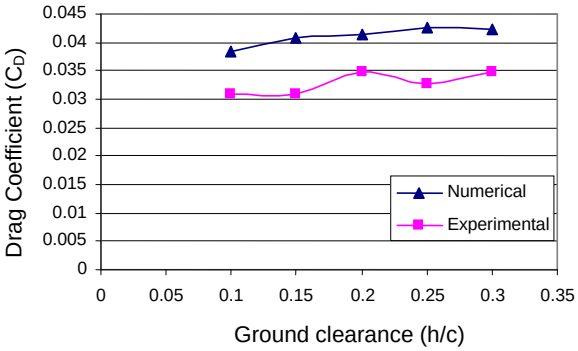


Figure 5: Drag coefficient ($C_D$) versus ground clearance (h/c) for angle of attack 2º and AR = 1.5.

### 3.3 Lift to Drag Ratio (L/D)

Lift to drag ratio from numerical simulations and experimental data [4] are shown in Tables 4 and Figure 6. Generally, the trend of lift to drag ratio of the numerical method has an approximate agreement with experiments. Moreover, both simulations demonstrate lift to drag ratio increases with smaller ground clearance.

Table 4. Lift to drag ratio versus ground clearance with angle of attack 2º and AR = 1.5 for experimental and numerical result.

| Ground clearance | Numerical | Experimental |
|---|---|---|
| 0.1 | 9.743 | 12.903 |
| 0.15 | 8.741 | 12.742 |
| 0.2 | 8.228 | 10.571 |
| 0.25 | 7.969 | 11.212 |
| 0.3 | 7.749 | 10.571 |

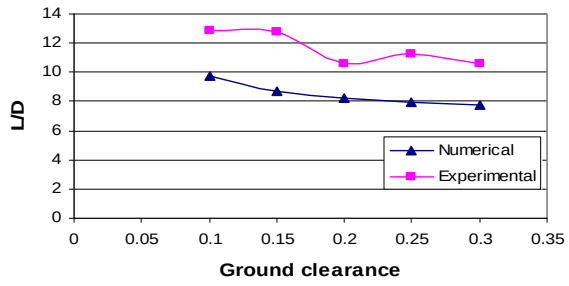


Figure 6: Lift to drag ratio (L/D) versus ground clearance (h/c) for angle of attack 2º and AR = 1.5.

### 3.4 Moment Coefficient ($C_M$) and Center of Pressure ($X_{cp}$)

The small variation of moment coefficient for present numerical results and experimental data [6] versus ground clearance is shown in Table 5. Also, Figure 7 confirms the good agreement between computational and experimental results of moment coefficient. According the data in Table 6 the center of pressure moved to lending edge as the ground clearance decreased for both methods. Furthermore, there is acceptable conformity for numerical method to determine center of pressure as shown in Figure 8.

Table 5. Moment coefficient versus ground clearance with angle of attack 2º an AR=1.5 for experimental and numerical result.

| Ground clearance | Numerical | Experimental |
|---|---|---|
| 0.1 | 0.0873 | 0.0700 |
| 0.15 | 0.0869 | 0.0760 |
| 0.2 | 0.0857 | 0.0753 |
| 0.25 | 0.0877 | 0.0748 |
| 0.3 | 0.0862 | 0.0783 |

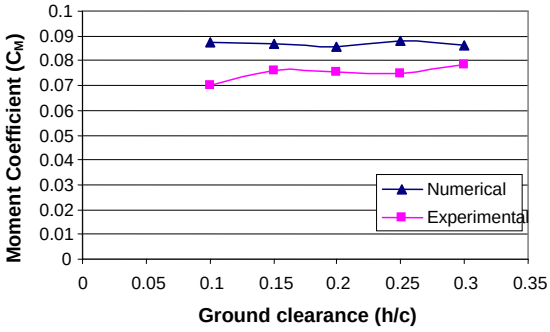


Figure 7: Moment coefficient ($C_M$) versus ground clearance for angle of attack 2º and AR = 1.5.

Table 6: Center of pressure versus ground clearance with angle of attack 2º and AR = 1.5 for experimental and numerical result.

| Ground clearance | Numerical | Experimental |
|---|---|---|
| 0.1 | 0.4826 | 0.4242 |
| 0.15 | 0.4928 | 0.4449 |
| 0.2 | 0.5000 | 0.4580 |
| 0.25 | 0.5079 | 0.4545 |
| 0.3 | 0.5114 | 0.4649 |

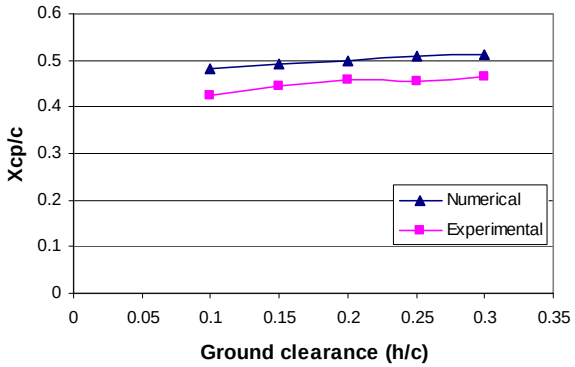


Figure 8: Center of pressure ($X_{CP}/c$) versus ground clearance for angle of attack 2º and AR = 1.5.

## 4. RESULTS AND DISCUSSION

The affect of taper reverse wing with negative dihedral angle of compound wing was exposed in Tables 7-11 and Figures 9-13. The results of lift coefficients versus ground clearance with angle of attack (AOA) 2º and aspect ratio 1.25 of rectangular wing and compound wing are shown in Figure 9. The increment of lift coefficient for compound wing is computed by Eq.4 in Table 7.There is considerable improvement on lift coefficient in small ground clearance for compound wing as compare with rectangular wing. It can see the increment of lift coefficient is 20.25% at ground clearance 0.1, However, a small reducing in lift coefficient appeared at higher ground clearance.

$$Icrement(\%) = \frac{C_{L(Compound)}}{C_{L(\mathrm{Re}c\tan gular)}} - 1 \qquad (4)$$

Table 7: Lift coefficient versus ground clearance with angle of attack 2º for rectangular and compound wing.

| Ground clearance | Rectangular | Compound | Increment of CL % |
|---|---|---|---|
| 0.1 | 0.3186 | 0.3831 | 20.25 |
| 0.15 | 0.3091 | 0.3178 | 2.80 |
| 0.2 | 0.3017 | 0.2953 | -2.14 |
| 0.25 | 0.2932 | 0.2834 | -3.35 |
| 0.3 | 0.2904 | 0.2728 | -6.08 |

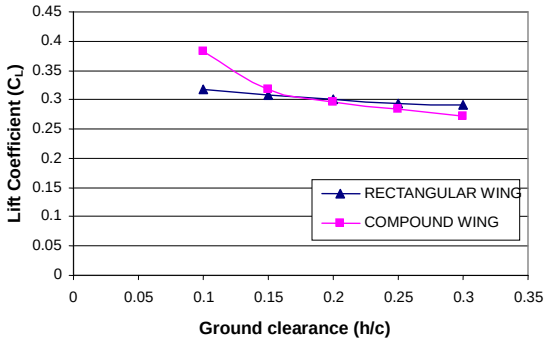


Figure.9: Lift coefficient ($C_L$) versus ground clearance for angle of attack2º.

The drag coefficients of rectangular and compound wing versus ground clearance with angle of attack 2º and aspect ratio 1.25 are depicted in Figure 10, in addition the reduction of drag coefficient for compound wing is calculated by Eq.5 in Table 8. This reduction is between 9-10.30% which the maximum reduction occurs in ground clearance 0.1.

$$\mathrm{Re}\,duction\,(\%) = 1 - \frac{C_{D(Compound)}}{C_{D(\mathrm{Re}c\tan gular)}} \qquad (5)$$

Table 8: Drag coefficient versus ground clearance with angle of attack 2º for rectangular and compound wing.

| Groud clearance | Rectangular | Compound | Reduction of CD % |
|---|---|---|---|
| 0.1 | 0.0332 | 0.0297 | 10.30 |
| 0.15 | 0.0347 | 0.0314 | 9.37 |
| 0.2 | 0.0353 | 0.0321 | 9.05 |
| 0.25 | 0.0355 | 0.0322 | 9.55 |
| 0.3 | 0.0358 | 0.0326 | 9.02 |

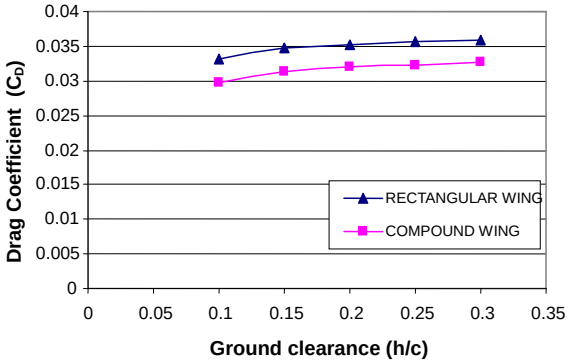


Figure 10: Drag coefficient ($C_D$) versus ground clearance for angle of attack2º.

The lift to drag ratio of rectangular and compound wing versus ground clearance for angle of attack 2º summarize in Table 9, in addition, the increment of lift to drag ratio of compound wing related to rectangular wing is determined by Eq.6. This increment in small ground clearance is so high where it is around 34% in ground clearance 0.1 that can be related to the high efficiency and saving energy of present wing. The trend of lift to drag ratio versus ground clearance for both wings is shown in Figure 11.

$$Increment\,(\%) = \frac{L/D_{(Compound)}}{L/D_{(\mathrm{Re}\,c\,\tan\,gle)}} - 1 \qquad (6)$$

Table 9: Lift to drag ratio versus ground clearance with angle of attack 2º for rectangular and compound wing.

| Grod clearane | Rectangular | Compound | Increment of L/D % |
|---|---|---|---|
| 0.1 | 9.606 | 12.877 | 34.06 |
| 0.15 | 8.920 | 10.118 | 13.43 |
| 0.2 | 8.550 | 9.199 | 7.59 |
| 0.25 | 8.249 | 8.814 | 6.86 |
| 0.3 | 8.109 | 8.371 | 3.23 |

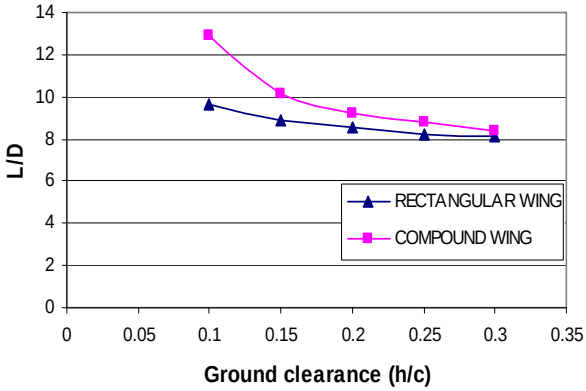


Figure 11: Lift to drag ratio (L/D) versus ground clearance for angle of attack2º.

The variation of moment coefficients for rectangular and compound wing versus ground clearance with angle of attack 2º and aspect ratio 1.25 are shown in Table 10 and Figure 12. A moment coefficient that causes a decreasing on angle of attack was named positive moment. The reduction of moment coefficient for compound wing is calculated by Eq.7 in Table 10. This reduction at extreme ground clearance (h/c=0.1) is small indicates the stability of compound wing has a little decline. The center of pressure of wing is another principal parameter for stability during take-off and landing conditions. Table 11 and Fig.13 illustrates the variation of center of pressure of both wings versus ground clearance. According to presented results the center of pressure of compound wing is a slight closer to leading edge of wing.

The resulted of positive moment coefficient decreases angle of attack.

$$\mathrm{Re}\,duction\,(\%) = 1 - \frac{C_{M(Compound)}}{C_{M(\mathrm{Re}\,c\,\tan\,gular)}} \qquad (7)$$

Table 10: Moment coefficient versus ground clearance with angle of attack 2º for rectangular and compound wing.

| Groud clearance | Rectanguar | Compound | Reduction of CM % |
|---|---|---|---|
| 0.1 | 0.0819 | 0.0778 | 4.94 |
| 0.15 | 0.0829 | 0.0716 | 13.63 |
| 0.2 | 0.0832 | 0.0703 | 15.56 |
| 0.25 | 0.0823 | 0.0699 | 15.01 |
| 0.3 | 0.0830 | 0.0688 | 17.15 |

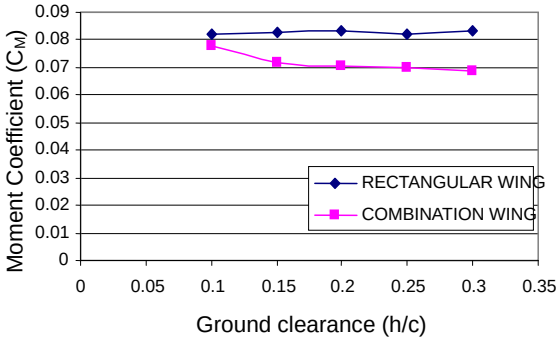


Figure.12: Moment coefficient ($C_M$) versus ground clearance for angle of attack2º.

Table 11: Center of pressure versus ground clearance with angle of attack 2º for rectangular and compound wing.

| Groud clearance | Rectanguar | Compound | Reduction of Xcp/c % |
|---|---|---|---|
| 0.1 | 0.5062 | 0.4527 | 10.57 |
| 0.15 | 0.5174 | 0.4748 | 8.24 |
| 0.2 | 0.5249 | 0.4873 | 7.17 |
| 0.25 | 0.5296 | 0.4960 | 6.35 |
| 0.3 | 0.5349 | 0.5013 | 6.27 |

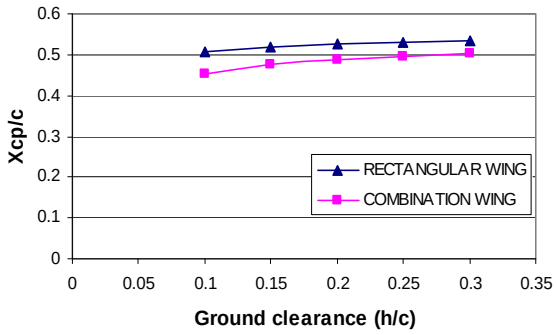


Figure 13: Center of pressure ($X_{CP}$/c) versus ground clearance for angle of attack2º.

## 5. CONCLUSION

The target of this research is to investigate the aerodynamic characteristics of an especial ram wing concept named compound wing. Based on the computational results the lift and drag coefficient of the compound wing has considerable modification as compare with rectangular wing for small ground clearance. The taper reverse wing with negative dihedral angle in the sides of compound creates a greater decreasing of down-wash velocity due to the ground effect that leads to a higher augmentation in lift and reduction of drag, as well as an increase of left to drag ratio for the wing. The high increment of lift to drag ratio for present wing in extreme ground effect (34%) is recognized a good efficiency for WIG craft. The moment coefficient has a little diminishing in lower ground clearance, also the center of pressure of present wing has a small shift forward to leading edge of wing as contrast with rectangular wing that can reduce the stability. A horizontal tail out of ground effect is one alternative to modify stability. For extra investigate, the aerodynamic characteristics and stability of present wing with horizontal tail wing will be numerically researched and compared with experimental data using UTM wind tunnel.

## ACKNOWLEDGEMENTS

The authors would like to thank the Ministry of Science, Technology, Innovation (MOSTI) Malaysia for funding this research under vote number 79344, and UTM due to high performance computing facility.

## REFERENCES

[1] Yun, L., Bliault, A., Doo, J., "WIG Craft and Ekranoplan:Ground Effect Craft Technology," *Springer Science+Business Media, LLC* (2010).

[2] Rozhdestvensky, K.-V., "Wing-in-ground effect vehicles," *Elsevier Journal of aerospace science*, Vol. 42, pp. 211-283 (2006).

[3] Chawla, M.-D., Edwards, L.-C., and Franke, M.-E., "Wind-tunnel investigation of wing-in-ground effect," *Journal of Aircraft*, Vol. 27, No. 4, pp. 289 (1990).

[4] Ahmed, M.-R., and Sharma, S.-D., "An investigation on the aerodynamics of a symmetrical airfoil in ground effect," *Elsevier Journal of Experimental Thermal and Fluid science*, Vol. 29, pp.633-647 (2004).

[5] Ahmed, M.-R., Takasaki, T., and Kohama, Y., "Aerodynamic of NACA4412 airfoil in ground effect," *AIAA Journal*, Vol. 45, No. 1, pp. 37 (2007).

[6] Jung, K.-H., Chun H.-H., and Kim, H.-J., "Experimenta investigation of wing-in-ground effect with a NACA 6409 section," *JASNAOE Mar Sci Technol*, Vol. 13, pp. 317-327 (2008).

[7] Chun, H.-H., and Chang, C.-H., "Turbulence flow simulation for wings in ground effect with two ground conditions: fixed and moving ground," *International Journal of maritime engineering*, pp.211-227 (2003).

[8] Moon, Y.-J., Oh, H.-J., and Seo, J.-H., "Aerodynamic investigation of three-dimensional wings in ground effect for aero-levitation electric vehicle," *Elsevier SAS Journal of Aerospace and Technology*, Vol. 9, pp. 485-494 (2005).

[9] Ockfen, A.-E., and Matveev, K.-I., "Aerodynamic characteristics of NACA4412 airfoil section with flap in extreme ground effect," *Inter J Nav Archit Oc Engng*, Vol. 1, pp. 1-12, (2009).

[10] Kirillovykh V.-N., "Russian ekranoplans," Proceedings of the international workshop on twenty-*first century flying ships*, pp. 71.117 (1995).